Available online at www.sciencedirect.com
SCIENCE DIRECT
Thermochimica Acta 436 (2005) 1–9
thermochimica acta
www.elsevier.com/locate/tca

Determination of solubility data by means of calorimetry

Dragomir Sapoundjiev [a,*], Heike Lorenz [a], Andreas Seidel-Morgenstern [a,b]

[a] *Max-Planck-Institut fuer Dynamik komplexer technischer Systeme, Sandtorstrasse 1, D-39106 Magdeburg, Germany*
[b] *Otto-von-Guericke-Universitaet, PSF 4120, D-39016 Magdeburg, Germany*

Received 1 October 2004; received in revised form 21 June 2005; accepted 23 June 2005
Available online 8 August 2005

Abstract

A calorimetric method for solubility determination is reported. A mathematical model is proposed to describe experimentally observed dissolution processes. The new technique allows the determination of the solubility curve in a wide temperature range by means of a single calorimetric run. The objective of the approach is not the high accuracy of the classical methods, but the minimization of experimental efforts. It is of particular interest for high-priced industrial products, e.g. pharmaceuticals or specialty chemicals. The method provides information about the dissolution kinetics and the dissolution heat as well. Based on solubility measurements carried out for various organic systems of fine chemicals, the experimental conditions affecting the solubility results are discussed in detail.

Keywords: Calorimetric approach; Solubility determination; Mathematical modelling; Organic systems; Application field

1. Introduction

Solubility data are essential for designing chemical processes, e.g. crystallization-based separations and chromatographic resolutions. However, there is a significant lack of solubility data with regard to new industrial products (e.g. pharmaceuticals) and specialty chemicals [1]. In addition, industrial systems frequently form polymorphs or involve impurities and the actual solubility is of particular importance [2]. Thus, efforts are devoted to obtain the required data with a minimum time and substance consumption.

Solubilities can be obtained by performing either calculations or measurements. The prediction of solubilities is restricted by availability of thermodynamic data of pure components and activity coefficient values [3–6]. Generally, solubility measurements are more reliable than calculated data [7].

Two basic techniques are available to measure solid/liquid equilibria (SLE)—isothermal and polythermal techniques. In both cases, different classical methods have been established [8]. For example, to apply the polythermal method, a solvent–solute mixture of known composition containing an excess of solid is prepared. Subsequently, the solution is heated at different heating rates to dissolve the solute. The temperature when the last crystals disappear is detected by visual observation or by monitoring a concentration-dependent physical or physicochemical property (refractive index, conductivity, particle size distribution, etc.) [8]. The solubility temperature is derived by extrapolating the detected temperatures to a heating rate of zero.

To reduce the experimental time and sample amount, innovative calorimetric techniques have been developed where the heat effect caused by dissolution is applied to detect the solubility temperature. Castronuovo et al. [9] presented an isothermal approach to derive simultaneously solubility, dissolution and dilution enthalpies. Complex ternary phase diagrams with regard to their phase-transition lines are determined via a quasiisothermal thermometric technique [10]. A theoretical analysis and a mathematical modelling of the method are provided in [11].

A quite novel application of DSC is the polythermal investigation of solubility equilibria. Young and Schall [12] presented solubility measurements of cycloalkanes in organic solvents by means of a multi-cell DSC. Applying the polythermal method, Lorenz and Seidel-Morgenstern [13] and

* Corresponding author. Tel.: +49 391 6110 287; fax: +49 391 6110 635.
E-mail address: dragomir@mpi-magdeburg.mpg.de (D. Sapoundjiev).

0040-6031/$ – see front matter © 2005 Elsevier B.V. All rights reserved.
doi:10.1016/j.tca.2005.06.031

Mohan et al. [14] studied the parameters affecting the solubility determination and tested the technique systematically for several organic systems in different aqueous and non-aqueous solvents. Recently, solubility measurements of less stable organic polymorphs in water were shown [15].

In the present article, a calorimetric approach to obtain solubility data based on the method proposed in [13,14] is reported. The novelty is that the calorimetric data recorded during the dissolution process are converted into a solubility curve covering a wide temperature range. Thus, contrary to the methods described before, not only the end of dissolution is taken as an estimate for the solubility temperature, but the whole thermal effect is applied to obtain the solubility curve as a function of temperature. A special focus is devoted to the mathematical description of the calorimetric experiment with the objective of interpreting the heat-flow signal. A detailed analysis, both from theoretical point of view and from the experimental background, is performed with respect to the parameters affecting the solubility determination.

The approach is applied to a pharmaceutical intermediate, adipic acid, mandelic acid, glycine, D-xylose and DL-threonine in different solvents.

2. Experimental

2.1. Equipment

Calorimetric experiments were performed by a SETARAM DSC 111 and a SETARAM Differential Reaction Calorimeter (DRC).

The DSC 111 is a Calvet-type heat-flux calorimeter, where the sample and the reference crucible are completely surrounded by thermopiles. The main advantage of DSC consists in the particularly small sample amounts required. An obvious drawback is the absence of stirring, making solubility measurements impossible for systems with severe mass and heat-transfer limitations. More detailed calorimeter specifications with regard to solubility measurements are given in [13].

The DRC is based on two double-jacketed vessels acting as a sample and a reference. A fluid circulating in the jackets provides an equal ambient temperature for both vessels. The calorimetric principle is based on the continuous measurement of the temperature difference between the two vessels during the experiment. To correlate the temperature difference to the heat flow, a Joule-effect calibration is applied. Active stirring insures better heat and mass transfer than in the DSC. A detailed device description and different operation modes of the apparatus are given in [16,17].

2.2. Materials

The systems and the experimental conditions for solubility determination are summarized in Table 1. Adipic acid, mandelic acid, glycine and DL-threonine were obtained from Aldrich or Merck with purity >99%. The water used as solvent was deionized and acetonitrile was of HPLC grade. The solubility of D-xylose (purity >99%) was studied in a solvent mixture with a composition given in Table 1. The D-xylose and the pharmaceutical intermediate (called further component A) were supplied from Nordzucker AG (Braunschweig) and Schering AG (Berlin), respectively.

2.3. Procedure for solubility measurement

A sample of known quantities of solvent and solid is prepared in the calorimetric vessel. The slurry is heated up primarily until obtaining clear solution and maintained at the high temperature for at least 1 h. Subsequently, the sample is cooled to the initial temperature and partly recrystallized. Then the solution is equilibrated until the baseline line is constant, normally 6–7 h. This pretreatment is of particular importance to provide fine crystals and an equal crystal-size distribution at the beginning of every heating run. Afterwards, the sample is subjected to a constant heating rate and the temperature difference between the two vessels is recorded.

3. Mathematical description of the calorimetric experiments

3.1. Modelling

The derived model plays a key role in the development and understanding of the method proposed here.

Mass and enthalpy balances are formulated for the two vessels (sample and reference). The following assumptions

Table 1
Solid–solvent systems used for solubility determination and experimental conditions

Systems		Apparatus	Temperature range (°C)	Heating rate (K/min)	Concentration range (wt.%)	Sample amount (g)
Solid	Solvent					
Compound A	Acetonitrile	DSC 111	10–90	0.25–8	36.8–72.5	0.05–0.11
Adipic acid	Water	DRC	5–70	0.2–1.5	9–15	80
Mandelic acid	Water	DRC, DSC 111	5–75	0.2–2.5	10–80	80–160
Glycine	Water	DRC	5–80	0.35–1	20–30	150–220
D-Xylose	Sugar matrix[a]	DRC	20–50	0.2–1	45–65	75–120
DL-Threonine	Water	DRC	10–60	0.5–1.5	20–22	75–90

[a] Sugar matrix: 50 wt.% water, 18.8 wt.% arabinose, 15.35 wt.% glucose, 10.6 wt.% galactose, 3.5 wt.% mannose, 1.75 wt.% rhamnose.

are made:

1. The vessels behave identically. Thus, only the internal volumes are considered.
2. The heat-transfer coefficients of the sample and reference vessels are equal.
3. There are no temperature or concentration gradients in the solution.
4. Linear heating rates, β, are chosen, i.e.:

$$\frac{dT}{dt} = \beta \tag{1}$$

5. The applied heating rates are small enough to approximate equilibrium conditions. Thus, at any temperature, the solution concentration is equal to the saturation concentration.
6. The solubility increases with rising temperature.

3.1.1. Sample vessel

3.1.1.1. Mass balance. Since the total sample mass $m_{\text{total}}^{\text{sample}}$ is constant,

$$\frac{dm_{\text{total}}^{\text{sample}}}{dt} = 0 = \frac{dm_{\text{solvent}}}{dt} + \frac{dm_{\text{solute}}}{dt} + \frac{dm_{\text{solid}}}{dt} \tag{2}$$

where m_{solvent}, m_{solute} and m_{solid} are the masses of solvent, solute and undissolved solid, respectively. The solvent mass does not change during an experiment, so the first term on the right hand of Eq. (2) is zero.

The solubility, S, is defined as:

$$S = \frac{m_{\text{solute}}}{m_{\text{solvent}}} \tag{3}$$

Based on assumption 5, the solute in the liquid phase corresponds to the equilibrium solubility. Thus, rearranging Eq. (2) and considering the linear heating rate β (Eq. (1)), we get:

$$m_{\text{solvent}}\frac{dS}{dt} + \frac{dm_{\text{solid}}}{dt} = 0 \tag{4}$$

Using a linear heating rate (Eq. (1)) analogously holds:

$$m_{\text{solvent}}\frac{dS}{dT} + \frac{dm_{\text{solid}}}{dT} = 0 \tag{4a}$$

3.1.1.2. Enthalpy balance. In the sample vessel, an enthalpy balance for the liquid phase consisting of saturated solution (solvent plus solute, with enthalpy H_{solution}), the solid phase (undissolved crystals, with enthalpy H_{solid}) and the heat flux due to dissolution ($\dot{H}_{\text{dissolution}}$) are considered, as well as the heat flow $\dot{H}_{\text{add. effects}}$ which could be generated by further thermal phenomena (decomposition, polymorphic transition, solvent evaporation, etc.). Thus, the balance leads to:

$$\frac{dH^{\text{sample}}}{dT} = \frac{dH_{\text{solution}}}{dT} + \frac{dH_{\text{solid}}}{dT} + \frac{\dot{H}_{\text{dissolution}}}{\beta} + \frac{\dot{H}_{\text{add. effects}}}{\beta} \tag{5}$$

For the two temperature-dependent enthalpies H_{solution} and H_{solid} holds:

$$H_{\text{solution}}(T) = \left(h_{\text{solution}}^0 + \int_{T_0}^{T} \overline{C}p_{\text{solution}}(T)\,dT\right) m_{\text{solution}}(T) \tag{6}$$

and

$$H_{\text{solid}}(T) = \left(h_{\text{solid}}^0 + \int_{T_0}^{T} Cp_{\text{solid}}(T)\,dT\right) m_{\text{solid}}(T) \tag{7}$$

where h_{solution}^0 and h_{solid}^0 are enthalpies at the reference temperature T^0, $\overline{Cp}_{\text{solution}}$ and Cp_{solid} are heat capacities of solution and solid, respectively. As a further simplification, the heat capacity of the solution $\overline{Cp}_{\text{solution}}$ is taken only as temperature function for a "mean" solution concentration. The validity of this assumption will be shown in Section 3.2.

Considering the temperature dependency of the enthalpies, relating the dissolution effect to the change of solid mass and neglecting additional thermal effects, for $T = T^{\text{sample}}$ holds:

$$\left.\frac{dH^{\text{sample}}}{dT}\right|_{T^{\text{sample}}} = \frac{d}{dT}\left[\left(h_{\text{solution}}^0 + \int_{T_0}^{T^{\text{sample}}} \overline{C}p_{\text{solution}}(T)\,dT\right) m_{\text{solution}}(T^{\text{sample}}) + \left(h_{\text{solid}}^0 + \int_{T_0}^{T^{\text{sample}}} Cp_{\text{solid}}(T)\,dT\right) m_{\text{solid}}(T^{\text{sample}})\right] + \overline{h}_{\text{dissolution}}\left.\frac{dm_{\text{solid}}}{dT}\right|_{T^{\text{sample}}} \tag{8}$$

In Eq. (8), the specific $\overline{h}_{\text{dissolution}}$ represents a dissolution enthalpy for infinite dilution at the reference temperature T^0. Thus, possible effects of temperature and composition are neglected.

Rearranging Eq. (8) leads to:

$$\begin{aligned}\left.\frac{dH^{\text{sample}}}{dT}\right|_{T^{\text{sample}}} &= h_{\text{solution}}^0 \left.\frac{dm_{\text{solution}}}{dT}\right|_{T^{\text{sample}}} + \overline{C}p_{\text{solution}}(T^{\text{sample}})m_{\text{solution}}(T^{\text{sample}}) \\ &+ \int_{T_0}^{T^{\text{sample}}} \overline{C}p_{\text{solution}}(T)\,dT \left.\frac{dm_{\text{solution}}}{dT}\right|_{T^{\text{sample}}} \\ &+ h_{\text{solid}}^0 \left.\frac{dm_{\text{solid}}}{dT}\right|_{T^{\text{sample}}} + Cp_{\text{solid}}(T^{\text{sample}})m_{\text{solid}}(T^{\text{sample}})\end{aligned}$$

$$+\int_{T_0}^{T^{\text{sample}}} Cp_{\text{solid}}(T)\,\mathrm{d}T\,\frac{\mathrm{d}m_{\text{solid}}}{\mathrm{d}T}\bigg|_{T^{\text{sample}}} + \overline{h}_{\text{dissolution}}\,\frac{\mathrm{d}m_{\text{solid}}}{\mathrm{d}T}\bigg|_{T^{\text{sample}}} \quad (9)$$

From the mass balance, Eqs. (2) and (4a) can be derived:

$$\frac{\mathrm{d}m_{\text{solution}}}{\mathrm{d}T} = -\frac{\mathrm{d}m_{\text{solid}}}{\mathrm{d}T} = m_{\text{solvent}}\frac{\mathrm{d}S}{\mathrm{d}T} \quad (10)$$

Combining Eqs. (9) and (10) provides:

$$\begin{aligned}\frac{\mathrm{d}H^{\text{sample}}}{\mathrm{d}T} &= \left(h^0_{\text{solution}} + \int_{T_0}^{T^{\text{sample}}} \overline{C}p_{\text{solution}}(T)\,\mathrm{d}T - h^0_{\text{solid}} - \int_{T_0}^{T^{\text{sample}}} Cp_{\text{solid}}(T)\,\mathrm{d}T - \overline{h}_{\text{dissolution}}\right) m^{\text{sample}}_{\text{solvent}} \times \frac{\mathrm{d}S}{\mathrm{d}T}\bigg|_{T^{\text{sample}}} + \overline{C}p_{\text{solution}}(T^{\text{sample}})m_{\text{solution}}(T^{\text{sample}}) \\ &\quad + Cp_{\text{solid}}(T^{\text{sample}})m_{\text{solid}}(T^{\text{sample}}) \quad (11)\end{aligned}$$

3.1.2. Reference vessel

3.1.2.1. Mass balance. The reference vessel is filled only with pure solvent. Thus, the mass change is given by:

$$\frac{\mathrm{d}m^{\text{ref}}_{\text{total}}}{\mathrm{d}T} = \frac{\mathrm{d}m^{\text{ref}}_{\text{solvent}}}{\mathrm{d}T} = 0 \quad (12)$$

3.1.2.2. Enthalpy balance. The enthalpy change in the reference vessel due to the temperature rise is:

$$\frac{\mathrm{d}H^{\text{ref}}}{\mathrm{d}T} = \frac{\mathrm{d}H_{\text{solvent}}}{\mathrm{d}T} \quad (13)$$

Considering in analogy to Eqs. (6) and (7), the temperature dependency of the enthalpy, for $T = T^{\text{ref}}$ holds:

$$\frac{\mathrm{d}H^{\text{ref}}}{\mathrm{d}T}\bigg|_{T^{\text{ref}}} = Cp_{\text{solvent}}(T^{\text{ref}})m^{\text{ref}}_{\text{solvent}} \quad (14)$$

where Cp_{solvent} is the heat capacity of the solvent.

3.1.3. Heat flow between sample and reference vessel

According to assumptions 1, 2, 3 and 5, the temperatures in the sample and reference vessels should be nearly equal during the heating run, i.e. $T^{\text{sample}} \approx T^{\text{ref}} \approx T$. Then the difference of the enthalpy derivatives with respect to temperature between the sample and the reference vessels is:

$$\frac{\mathrm{d}H^{\text{difference}}}{\mathrm{d}T}\bigg|_T = \frac{\mathrm{d}H^{\text{ref}}}{\mathrm{d}T}\bigg|_T - \frac{\mathrm{d}H^{\text{sample}}}{\mathrm{d}T}\bigg|_T \quad (15)$$

$\mathrm{d}H^{\text{difference}}/\mathrm{d}T$ corresponds to the measurable modified "heat flow" $\dot{H}^{\text{difference}}$(in J/K). Based on Eqs. (11), (14) and (15), an expression for this quantity can be derived:

$$\begin{aligned}\dot{H}^{\text{difference}}(T) &= Cp_{\text{solvent}}(T)m^{\text{ref}}_{\text{solvent}} + \left(-h^0_{\text{solution}} - \int_{T_0}^{T} \overline{C}p_{\text{solution}}(T)\,\mathrm{d}T + h^0_{\text{solid}} + \int_{T_0}^{T} Cp_{\text{solid}}(T)\,\mathrm{d}T + \overline{h}_{\text{dissolution}}\right) m^{\text{sample}}_{\text{solvent}}\frac{\mathrm{d}S}{\mathrm{d}T}\bigg|_T - \overline{C}p_{\text{solution}}(T)m_{\text{solution}}(T) - Cp_{\text{solid}}(T)m_{\text{solid}}(T) \quad (16)\end{aligned}$$

This equation predicts modified heat flows as a function of the temperature. Usage of Eq. (16) is a complicated task because all parameters must be known, i.e. heat capacities of solvent, solid and solution, standard enthalpies of solid and solution, dissolution enthalpy, solubility function and quantities of applied components. The following approximation leads to a simplified calculation.

The enthalpy difference between the solid and the solution phase is often smaller than the dissolution heat and can be neglected, i.e.:

$$\left|-h^0_{\text{solution}} - \int_{T_0}^{T} \overline{C}p_{\text{solution}}(T)\,\mathrm{d}T + h^0_{\text{solid}} + \int_{T_0}^{T} Cp_{\text{solid}}(T)\,\mathrm{d}T\right| \ll \left|\overline{h}_{\text{dissolution}}\right| \quad (17)$$

This is a critical assumption that needs to be verified in each specific case.

The simplified equation describing the modified heat flow is:

$$\begin{aligned}\dot{H}^{\text{difference}}(T) &= Cp_{\text{solvent}}(T)m^{\text{ref}}_{\text{solvent}} + \overline{h}_{\text{dissolution}}m^{\text{sample}}_{\text{solvent}}\frac{\mathrm{d}S}{\mathrm{d}T}\bigg|_T - \overline{C}p_{\text{solution}}(T)m_{\text{solution}}(T) - Cp_{\text{solid}}(T)m_{\text{solid}}(T) \quad (18)\end{aligned}$$

To further simplify the correlation between the solubility function and the heat flow, the terms containing heat capacity functions are neglected as their contribution is typically small compared to the dissolution effect. This assumption will be discussed in Section 3.2. Then instead of Eq. (18), a very simple equation is obtained:

$$\dot{H}_{\text{dissolution}}(T) = \overline{h}_{\text{dissolution}}m^{\text{sample}}_{\text{solvent}}\frac{\mathrm{d}S}{\mathrm{d}T}\bigg|_T \quad (19)$$

Table 2
Experimental and thermodynamic data on the water–racemic mandelic acid system for calculation of the calorimetric curves in Figs. 1–3 (solubility data (S) are taken from [22]; heat capacity data ($Cp_{\text{solution/solid}}$) were measured in our laboratory; dissolution enthalpy ($\bar{h}_{\text{dissolution}}$) is found in [21]; m_{MA} is the total quantity of mandelic acid in the sample; x is the solid concentration in the solution in g/g; T is temperature in °C)

m_{MA} (g)	$m^{\text{sample}}_{\text{solvent}}$ (g)	$m^{\text{ref}}_{\text{solvent}}$ (g)	$h_{\text{dissolution}}$ (J/g)	$S(T)$ (g/g)	Cp_{solution} (J/g K)	$\overline{Cp}_{\text{solution}}$ (J/g K)	Cp_{solvent} (J/g K)	Cp_{solid} (J/g K)
50	60	100	84.9	$3.68\times10^{-3}T^2 - 0.1819T + 2.4789$ T = 20–40	$-0.9724x + 4.0872$ x = 0.2–0.8	3.6 x = 0.5	4.18 T = 0–100	$4.3\times10^{-3}T + 0.9483$ T = 20–100

3.1.4. Solubility curve

Integration of Eq. (19) from T_1 to a higher temperature T_2 provides:

$$H^{1-2}_{\text{dissolution}} = \int_{T_1}^{T_2} \dot{H}_{\text{dissolution}}(T)\,\mathrm{d}T = \bar{h}_{\text{dissolution}} m^{\text{sample}}_{\text{solvent}}(S(T_2) - S(T_1)) \quad (20)$$

Assuming the solid is completely dissolved at $T_{\text{end, diss}}$ and $T_{\text{end, diss}} \geq T_2$, the overall heat due to dissolution of the solid at T_1 ($m_{\text{solid}}(T_1)$) in the temperature range T_1–$T_{\text{end, diss}}$ is:

$$H^{1-\text{end, diss}}_{\text{dissolution}} = \bar{h}_{\text{dissolution}} m_{\text{solid}}(T_1) \quad (21)$$

Dividing Eq. (20) by Eq. (21) provides:

$$\frac{H^{1-2}_{\text{dissolution}}}{H^{1-\text{end, diss}}_{\text{dissolution}}} = \frac{m^{\text{sample}}_{\text{solvent}}(S(T_2) - S(T_1))}{m_{\text{solid}}(T_1)} \quad (22)$$

Rearranging Eq. (22) yields finally the following equation allowing to determine the solubility curve based on calorimetric data in the temperature range T_1–$T_{\text{end, diss}}$:

$$S(T_2) = S(T_1) + \frac{H^{1-2}_{\text{dissolution}}}{H^{1-\text{end, diss}}_{\text{dissolution}}} \frac{m_{\text{solid}}(T_1)}{m^{\text{sample}}_{\text{solvent}}} \quad (23)$$

Eq. (23) is directly applicable to determine the solubility function if the solubility at T_1 ($S(T_1)$) is known from an independent measurement.

3.2. Analysis of thermodynamic parameters in the model

A parameter analysis is performed to estimate their influence on the predicted heat flow. The dissolution process of racemic mandelic acid in water is considered as an example. The calculations are performed for a 45 wt.% sample at a heating rate of 0.5 K/min. The data used are summarized in Table 2.

Initially, the impact of the concentration on the heat capacity of the solution is estimated. For that purpose, heat capacities of different mixtures of racemic mandelic acid in water were measured with the DRC at different temperatures. The results (not presented here) show that Cp for a given concentration remains nearly constant (±3%) within a temperature range of 30–40 K. Therefore, the effect of temperature can be neglected and the heat capacity can be expressed as a function of only composition as found for other organic compounds in aqueous solutions [18,19]. Neglecting the influence either of the temperature or of the concentration on the heat capacity are quite acceptable in narrow temperature/concentration intervals. Using both the measured heat capacity as a function of the concentration and the heat capacity as a constant for a "mean" concentration, calculations of the heat flow (Eq. (18)) were performed (not presented here). The results demonstrated that the approximation $\overline{Cp}_{\text{solution}} = f(T)$ is justified.

The influence of neglecting the heat capacities on the heat-flow curve is evaluated in Fig. 1. The calculations were performed using Eqs. (18) and (19) with the data from Table 2. The slopes between T_{start} and the peak maximum differ, which corresponds to different gradients of the solubility with temperature. The baseline at the beginning and at the end in the case of "pure dissolution" (Eq. (19)) becomes zero because the heat flow is caused only by the dissolution process. According to Eq. (18), there is a contribution to the heat flow due to the heat-capacity difference between the sample and the reference vessels resulting in a certain (non-zero) level of the measured signal at T_{start} and T_{end}, respectively (Fig. 1). The overall heat generated is similar in both cases which means that the thermal effect is mainly influenced by the heat of dissolution.

The impact of the standard dissolution enthalpy on the heat flow is discussed next. Such data are hardly available and frequently for prediction of solubility, the melting enthalpy of the pure solid is used instead of the dissolution enthalpy [20]. In Fig. 2, heat-flow curves predicted according to Eq. (18) with the dissolution enthalpy (data in Table 2) and the melting enthalpy (data from [22]) are presented. The calorimetric signal is strongly affected by the enthalpy value. In confor-

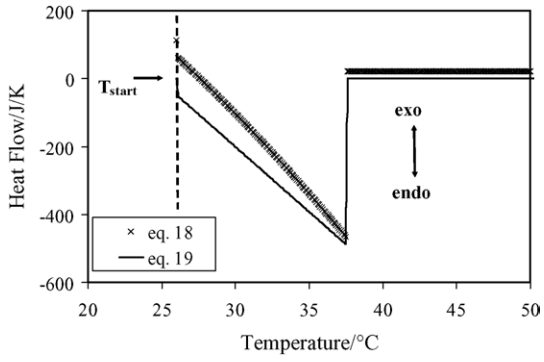

Fig. 1. Comparison between predicted heat flow using Eqs. (18) and (19).

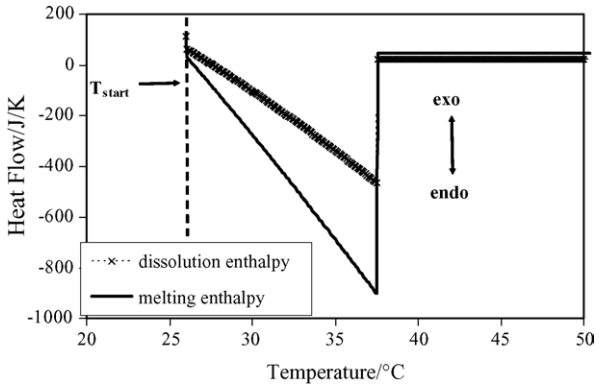

Fig. 2. Application of the melting and the dissolution enthalpy for calculation of the heat-flow curve (Eq. (18)).

mity with the values used, the difference in the absolute areas under the baseline is approximately twice. The slopes are also different which would imply different solubility functions. The baselines at the end are identical because the level corresponds just to the heat-capacity difference between sample and reference (Eq. (18)).

Generally, it can be concluded that mainly the dissolution process contributes to the strength of the calorimetric signal. The dissolution effect is determined by the change of the solubility with temperature (dS/dT) and the dissolution enthalpy ($\bar{h}_{\text{dissolution}}$) which affect the slope and the size of the calorimetric peak, respectively. As the impact of the heat capacity functions is not strongly pronounced, the simplifications used in this work to derive the equation for the solubility curve (Eq. (23)) are acceptable.

4. Results and discussion

4.1. Analysis of calorimetric experiments

In Fig. 3, the heat-flow curve obtained in a solubility measurement of racemic mandelic acid in water is compared with the predicted signal. The simplified calculation of the heat flow, based on Eq. (18), is performed mainly to support the understanding of the calorimetric data rather than to reproduce the experimental signal with high accuracy.

The sample is first equilibrated at the initial temperature (T_{start}). In the theoretical curve, the dissolution process starts immediately with the increase of the temperature. In the calorimetric experiment, there is a time lag due to heat-transfer limitations. As the solid starts to dissolve in the solvent, an enthalpy change due to the heat of dissolution is measured as a heat flow. The heat-flow curve is according to the theory proportional to the gradient of the solubility function (Eq. (18)). If the system is in equilibrium at every temperature, the last solid particles should dissolve at the solubility temperature (indicated by T_{sat} in Fig. 3) where the peak exhibits its maximum. Afterwards, the calculated curve reaches the baseline immediately and the heat flow is only due to the heat capacity difference between the sample and reference vessels. The peak maximum of the experimental curve appears at a temperature slightly higher than T_{sat}. The baseline line at the end is not reached promptly due to the sluggishness of the system. Generally, the shape of the predicted heat flow reproduces the experimental signal, although there is a shift of the theoretical baseline line due to the simplifications in the model. The "ideal" peak area representing the consumed heat matches well with the measured thermal effect between T_{start} and T_{sat}. The parallel course of the predicted thermogram and the calorimetric signal shows that the system is in quasi equilibrium during the controlled heating, i.e. assumption 5 is valid.

To understand the process in the calorimeter, the solution concentration was determined by refractometry during solubility experiments with racemic and (+)-mandelic acid in water. A result with (+)-mandelic acid is shown in Fig. 4. The solution concentration increases rapidly at T_1. The final concentration is reached at $T_{\text{end, diss}}$, higher then the peak maximum. The actual dissolution process in the temperature range T_1–$T_{\text{end, diss}}$ deviates from the theoretical prediction. Both temperatures can be determined from the derivative of

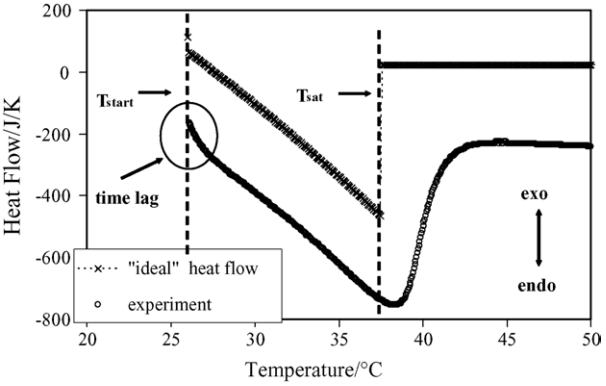

Fig. 3. Comparison between predicted (Eq. (18)) and experimental calorimetric curves for the sample 45 wt.% of racemic mandelic acid–water ($\beta = 0.5$ K/min).

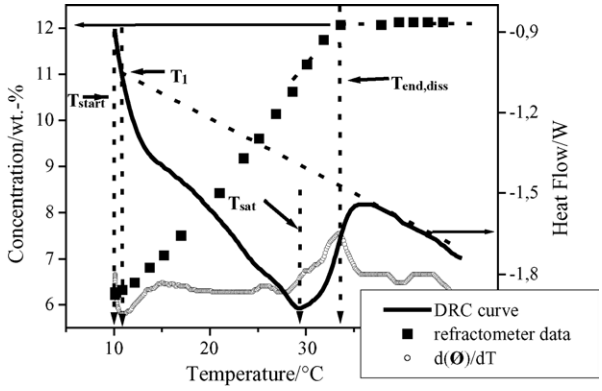

Fig. 4. Calorimetric measurement of 12 wt.% (+)-mandelic acid in water (DRC, sample: 80 g, $\beta = 0.5$ K/min) accompanied by online concentration analysis with refractometer (Ø = heat flow).

the calorimetric curve (dØ/dT in Fig. 4). The beginning as well as the end of the dissolution cause changes in the thermal signal which are indicated as points of inflection. The derivative of the heat flow exhibits minimum or maximum corresponding to T_1 and $T_{end,\ diss}$ from the concentration measurements. A measurement with racemic mandelic acid in water was recorded to observe visually when the last crystals vanish into the solution. While there was considerable undissolved material at T_{sat}, a clear solution was formed at $T_{end,\ diss}$.

Based on the theoretical and experimental analysis performed, the solubility function can be obtained applying Eq. (23) in the temperature interval T_1–$T_{end,\ diss}$ where both temperatures are the inflection points of the derivative of the calorimetric curve.

4.2. Influence of heating rate

As solubility is an equilibrium quantity, an infinitely low heating rate would keep the solution at equilibrium. However, such procedure is not useful because of time constraints and because it diminishes the amplitude of the thermal effect. A compromise has to be made between measuring sufficient heat effects in reasonable time and the accuracy of solubility results. As dissolution kinetics vary from system to system, an appropriate heating rate must be determined for every system.

The impact of the heating rate on the solubility results is demonstrated for a 15 wt.% sample of adipic acid in water at heating rates between 0.2 and 1.5 K/min (Fig. 5). The curves show similar shapes and distinct thermal effects. The absolute consumed heat is equal for every heating rate, but the measurable heat flux decreases at lower heating rates. The final dissolution temperatures ($T_{end,\ diss}$) differ only slightly. The derived solubility curves using Eq. (23) are presented in Fig. 5b in comparison with data obtained by means of the isothermal technique described in [22]. The initial solubility value ($S(T_1)$) was determined by interpolation of the isothermal data. The approximation of the isothermal solubilities is satisfying with average deviation less than 7%. All heating rates provide similar solubility results over a broad temperature interval >45 K. Dissolution kinetics are apparently sufficiently fast to allow these heating rates. Even the highest applied heating rate of 1.5 K/min is quite acceptable for measuring solubilities. The solubility curve in this temperature range is obtained by means of a single experiment, considerably reducing the experimental work.

4.3. Influence of concentration

In Fig. 6a, DSC curves for samples with different concentrations of component A in acetonitrile are presented. The sharp peak shapes indicate that dissolution is the main heat effect. With increasing concentration, the peak areas become larger and the final dissolution temperature appears at higher values. Hence, a positive slope of the solubility curve is expected. Fig. 6b presents the solubility curves determined by means of Eq. (23). Samples with a higher difference between final and initial solution concentration provide larger arcs of the solubility curves. Simultaneously, the accuracy declines and the average deviation attains 25% at the highest concentration. In the case of compound A in acetonitrile, it can be concluded that DSC measurements of concentrated samples are capable of obtaining solubility curves in very broad temperature ranges. Thus, a reduction of the experimental efforts is achieved.

4.4. Additional thermal effects during dissolution

Solubility measurements of glycine in water are shown in Fig. 7 for 30 wt.% sample. The curves are of “nontypical” shape. At certain temperatures, e.g. at about 50 °C for the curve with 1 K/min heating rate, an exothermal effect overlays the dissolution process. Glycine can crystallize from aqueous solutions in two enantiotropic polymorphic forms, α-glycine and γ-glycine [24]. According to Ostwald’s rule of stages, the initially obtained form is the least stable one that

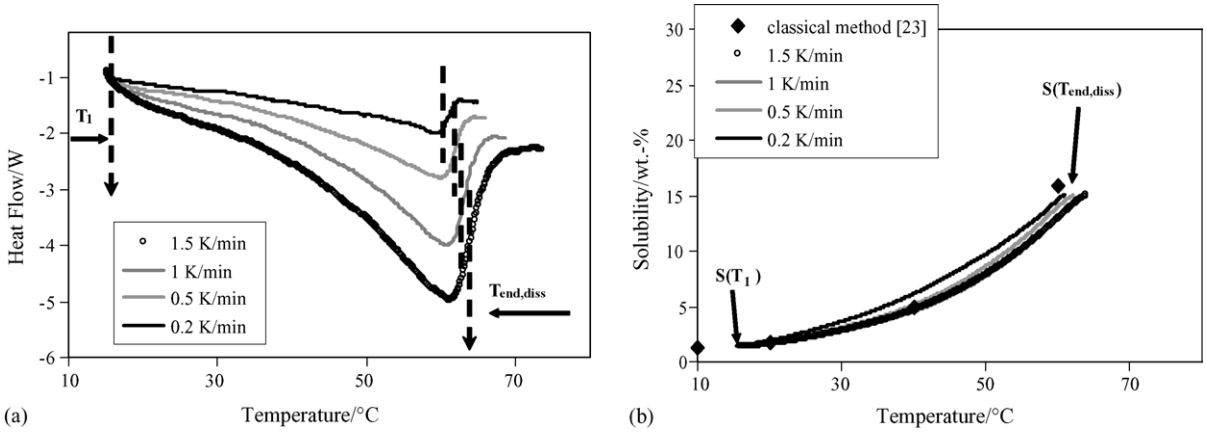

Fig. 5. (a) Heat-flow curves from solubility measurements at different heating rates (adipic acid in water, DRC, sample: 80 g, x = 15 wt.%). (b) Comparison between calculated solubility curves and literature data for adipic acid in water [23].

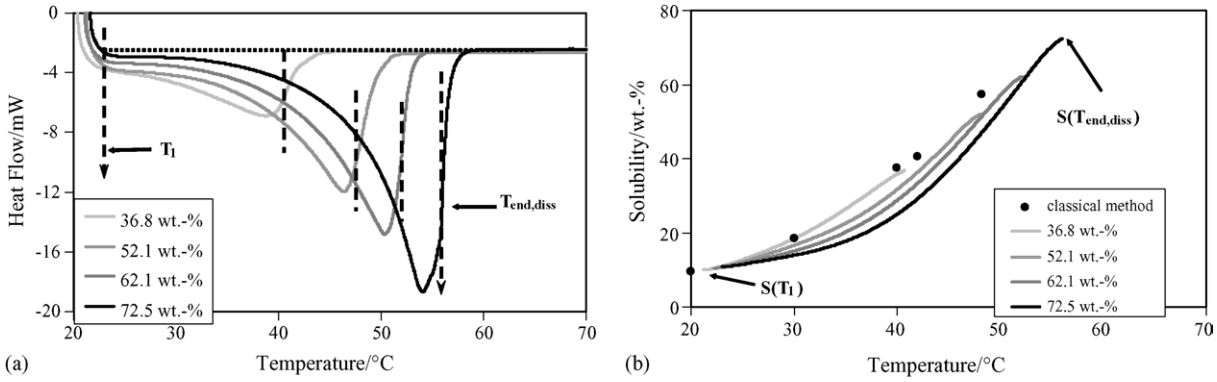

Fig. 6. (a) Heat-flow curves from DSC solubility experiments for different concentrations of compound A in acetonitrile (sample: 68–78 mg, $\beta = 1$ K/min). (b) Comparison between calculated solubility curves and data obtained independently by a classical isothermal method for component A in acetonitrile.

is closest in terms of free energy to the original state [25], i.e. usually the kinetically preferred α-glycine is spontaneously formed by rapid recrystallization [26]. For glycine–water mixtures with concentrations between 27 and 45 wt.%, phase transition from the α- into the γ-form is reported to take place in the temperature range between 40 and 80 °C depending on the experimental conditions [27]. Thus, the exothermal effects obtained (Fig. 7) might be due to the transition from the unstable α- into the stable γ-glycine. However, clarification of the phenomenon requires further experimental work.

Such additional information is valuable for assessing the crystallization behavior which is not provided by classical techniques. There, phase analysis is commonly performed at the end of the experiment.

4.5. Reproducibility

The reproducibility of the proposed method is studied by five measurements with racemic mandelic acid in water carried out in the DRC under the same experimental conditions (sample: 81 g, $x = 13$ wt.%, $\beta = 0.5$ K/min). The deviation between the calorimetric signals, as well as between the corresponding solubility curves is negligible.

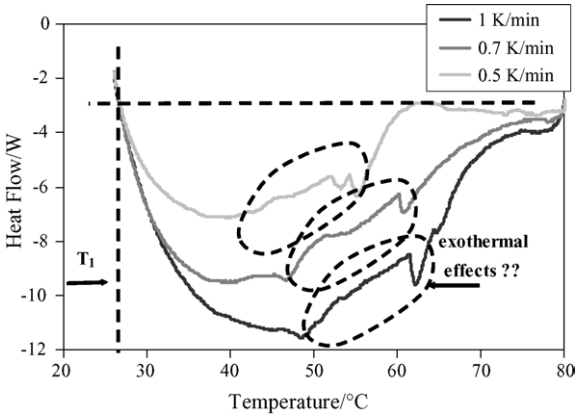

Fig. 7. Heat-flow curves of solubility measurements of glycine in water applying different heating rates (sample mass: 214 g, $x = 30$ wt.%).

4.6. Limitations

Limitations of the calorimetric approach are discussed for the two systems—D-xylose and DL-threonine. Measurements performed with D-xylose in a solvent mixture (Table 1) revealed that the heat effect caused by recrystallization in the pretreatment step was not identifiable because of very slow crystallization kinetics. Hence, it was not possible to determine whether the solution was in equilibrium before starting the heating cycle. That hindrance makes the calorimetric method inapplicable for systems with "slow" crystallization kinetics.

Another limitation of the approach is demonstrated for the system DL-threonine in water, a system where the increase of the solubility with temperature is only slight as is the dissolution rate [28,29]. The tiny and unclear thermal effects obtained could not be used to determine the solubility function. Therefore, the method is not applicable to systems with "slow" dissolution kinetics or a "weak" temperature dependence of the solubility. An absolute increase in solubility of at least 3 wt.% within 10 K is required to measure dissolution effects.

5. Conclusions

The accuracy of the proposed calorimetric approach depends on heating rate, dissolution rate, and the amount of solid in the sample. The main goal of the technique is fast acquisition of the solubility curve. The method cannot substitute classical measurements, but rather can be applied for a preliminary study of solid/liquid equilibria over a wide temperature range. For the systems and the experimental conditions used in this study, the maximum deviation from equilibrium data was approximately 12%.

The model derived supports the understanding of the dissolution process and provides a correlation between the measured heat flow and the solubility. This approach also gives information on the gradient of the solubility curve, the dissolution rate and on the magnitude of the heat accompanied

the dissolution. Furthermore, it is possible to obtain initial information concerning the general dissolution and recrystallization behavior.

Thus, the method is of particular interest for studying new substances or pharmaceutical intermediates in the early stage of development.

Heating rates between 0.5 and 1.5 K/min generally produced satisfying results. Measuring with 2 or 3 different heating rates in this range gives an idea about the rate of approaching equilibrium.

A previous dissolution and recrystallization step is strongly recommended to provide uniform initial conditions.

Additional thermal effects observed during the crystallization/dissolution experiment can help to detect possible phase transitions.

Acknowledgement

The authors thank the German Ministry for Education and Research for financial support.

References

[1] A.S. Myerson, Handbook of Industrial Crystallization, Butterworth-Heinemann, London, 1992 (Chapter 1).
[2] W. Beckmann, Eng. Life Sci. 3 (2003) 113.
[3] S.M. Walas, Phase Equilibria in Chemical Engineering, Butterworth, Boston, 1985 (Chapter 4).
[4] J.M. Prausnitz, R.N. Lichtenthaler, E. Gomez de Azevedo, Molecular Thermodynamics of Fluid-Phase Equilibria, second ed., Prentice-Hall, Englewood Cliffs, NJ, 1986 (Chapter 6).
[5] T.C. Frank, J.R. Downey, S.K. Gupta, Chem. Eng. Prog. 95 (1999) 41.
[6] J. Gmehling, B. Kolbe, Thermodynamik, VCH, Weinheim, 1992 (Chapter 7).
[7] N.S. Tavare, Industrial crystallization—process simulation, in: Analysis and Design, Plenum Press, New York, 1995 (Chapter 2).
[8] J.W. Mullin, Crystallization, third ed., Butterworth-Heinemann, Oxford, 1997 (Chapter 3).
[9] G. Castronuovo, V. Elia, M. Niccoli, F. Velleca, Thermochim. Acta 320 (1998) 13.
[10] E.C. Tavares, S.I.S. Marcelino, O. Chiavone-Filho, C.P. Souza, Thermochim. Acta 328 (1999) 253.
[11] P. Marchand, L. Lefebvre, G. Perez, J.-J. Counioux, G. Coquerel, J. Therm. Anal. Cal. 68 (2002) 37.
[12] P.H. Young, C.A. Schall, Thermochim. Acta 367–368 (2001) 387.
[13] H. Lorenz, A. Seidel-Morgenstern, Thermochim. Acta 382 (2002) 129.
[14] R. Mohan, H. Lorenz, A.S. Myerson, Ind. Eng. Chem. Res. 41 (2002) 4854.
[15] K. Park, J.M.B. Evans, A.S. Myerson, Cryst. Growth Des. 3 (2003) 991.
[16] R. André, M. Giordano, C. Mathonat, R. Naumann, Thermochim. Acta 405 (2003) 43.
[17] R. André, L. Bou-Diab, P. Lerena, F. Stoessel, M. Giordano, C. Mathonat, Org. Process Res. Dev. 6 (2002) 915.
[18] R.G. Clarke, L. Hnědkovský, P.R. Tremaine, V. Majer, J. Phys. Chem. B 104 (2000) 11781.
[19] S. Cabani, G. Conti, E. Matteoli, A. Tani, J. Chem. Soc., Faraday Trans. I 73 (1977) 476.
[20] A. Mersmann, Crystallization Technology Handbook, Marcel Dekker, New York, 1995 (Chapter 4).
[21] R.H. Perry, D.W. Green, Perry's Chemical Engineers' Handbook, McGraw-Hill, New York, 1997 (Chapter 2).
[22] H. Lorenz, D. Sapoundjiev, A. Seidel-Morgenstern, J. Chem. Eng. Data 47 (2003) 1280.
[23] M. Rauls (BASF Ludwigshafen, Germany), Personal information, 2000.
[24] M. Matsumoto, H. Yajima, T. Handa, Bull. Chem. Soc. Jpn. 59 (1986) 3803.
[25] W. Ostwald, Z. Phys. Chem. 22 (1897) 289.
[26] G.L. Perlovich, L.K. Hansen, A. Bauer-Brandl, J. Therm. Anal. Cal. 66 (2001) 699.
[27] T. Suzuki, F. Franks, J. Chem. Soc. Faraday Trans. 89 (1993) 3283.
[28] T. Shiraiwa, M. Yamauchi, Y. Yamamoto, H. Kurokawa, Bull. Chem. Soc. Jpn. 63 (1990) 3296.
[29] V.M. Profir, M. Matsuoka, Colloids Surf. A: Physiochem. Eng. Aspects 164 (2000) 315.